05,10

Spontaneous formation of Cr_2S_3 phase inclusions in a two-dimensional layered semiconductor CrSBr

© D.L. Gusenkov[1,4], R.A. Valeev[2], V.P. Piskorskii[2], A.I. Chernov[3], R.B. Morgunov[1,2,4]

[1] Federal Research Center of Problems of Chemical Physics and Medicinal Chemistry RAS, Chernogolovka, Russia
[2] All-Russian Scientific Research Institute of Aviation Materials of the Research Center „Kurchatov Institute", Moscow, Russia
[3] Center of Photonics and Two-Dimensional Materials, Moscow Physics and Technology Institute, Dolgoprudny, Russia
[4] Sechenov First Moscow State Medical University, Ministry of Health of the Russian Federation, Moscow, Russia

E-mail: spintronics2022@yandex.ru

Received January 20, 2025
Revised January 20, 2025
Accepted January 21, 2025

Variations in the physical properties of two-dimensional semiconductors due to different growth conditions and random changes in stoichiometry are a problem for their use. We analyzed the chemical composition and physical properties of two commercially grown CrSBr samples and found differences in magnetic and optical properties that can be explained by crystal heterogeneity. A strong bromine deficiency was observed in one of the samples, which led to a shift in the critical transition temperature to the metamagnetic state from 132 K in the perfect sample to 120 K in the nonstoichiometric sample. The critical temperature of 120 K, as well as the local X-ray diffraction spectra, are consistent with the parameters characteristic of the Cr_2S_3 phase, which coexists with the primary CrSBr phase.

Keywords: two-dimensional semiconductors, stoichiometry, magnetic transition, Raman spectroscopy, X-ray fluorescence analysis, metamagnetism.

DOI: 10.61011/PSS.2025.02.60680.13-25

1. Introduction

Two-dimensional lamellar semiconductors, whose conducting atomic layers are bound by the Van der Waals forces, are promising systems for electronics. This class of materials has been well-known long ago, it is, together with graphene, attracts the attention of researchers by unusual electric transport properties associated with restricted dimension of electron gas [1–3]. Two-dimensional metals, semiconductors and superconductors were well-known in organic chemistry, where BEDT-TTF, BETS, DOEO molecules and other donor molecules consisting of aromatic cycles were used to prepare two-dimensional salts usually associated with the Coulomb interaction in ionic crystals [4,5]. Van der Waals two-dimensional crystals are much more functional objects because they are able to be disintegrated into individual layers up to the atomic thickness layers using a relatively simple disintegration technique [6]. Such layers are the basis for next generation transistors with zero effective weight of charge carriers and concentration of carriers controlled by gate voltage [7,8]. Though the optical and electrical properties of such semiconductors have been already studied in sufficient detail, they are of interest for nanometer-thick samples. One of the problems in using this group of materials is their instability, oxidation capability, nonstoichiometry that appears during crystal and film growth and storage.

Purchase of commercial crystals doesn't guarantee the specified chemical composition and structure of these crystals. In particular, 2D Semiconductors CrSBr crystals have considerable deviations of magnetic properties from those that correspond to this compound in the literature. These changes may be caused by technique variations and specific crystal storage conditions. Light elements in them are substituted with other elements or can evaporate from the crystal giving rise to inclusions with a different chemical composition.

The objective of this study was to establish the reasons why the properties of CrSBr crystals may deviate from those described in the literature and in the comparative analysis of chemical composition, magnetic and optical properties of two types of commercial CrSBr polycrystals.

2. Procedure and samples

Two types of commercial CrSBr crystals were used for the experiments. Sample 1 was purchased from „2D Semiconductors", and sample 2 was grown at „HQ graphene". „2D Semiconductors" crystals were grown by the chemical vapor transport (CVT) technique, where Cr, S and Br_2

gases were used. „HQ grapheme“ didn't provide a synthesis report. Prior to the analysis of properties, the samples were split mechanically to prevent the possible effect of the oxidized top layer. Thickness of the samples $\sim 0.1-1$ mm was much larger than 20 nm, which enabled us to neglect the features of this material consisting of few layers.

Chemical composition of the sample was determined by the X-ray fluorescence analysis (XFA) using the Spektroskan MAKS — GVM spectrometer. Magnetic measurements were performed using the SQUID MPMS 5XL Quantum Design magnetometer in the temperature range from 2 K to 300 K and in a magnetic field from 0 kOe to 50 kOe. Optical properties were studied using the Confotec NR500 532 nm Raman scattering spectrophotometer equipped with a $\times 40$ lens and 1800 lines/mm grid. Calibration of the instrument was performed using the reference Raman scattering spectrum (RS) of a Si sample with a typical 521.5 cm^{-1} peak.

3. Experimental findings and discussion

3.1. Chemical composition and atomic structure

Chemical composition of the crystals was determined by the X-ray fluorescence analysis (XFA). Figure 1, *a* and *b* shows the XFA spectra for samples 1 and 2, respectively. Sample 1 has a complex spectrum where other elements, besides the specified Cr, S and Br atoms, are also detected. The presence of Ca, C and O lines in the spectrum is explained by impurities in the measurement chamber that were subtracted when calculating the results according to the same measurements performed on other reference samples with known composition. Spectrum of sample 2 contains less lines. Results of the quantitative analysis of chemical element concentrations in both samples are shown in Tables 1 and 2. According to the structural formula, the samples shall have equal concentrations of all atoms. However, sample 1 has a considerable stoichiometry deviation due to the lack of bromine. Chemical composition of sample 2 corresponds to the specified composition.

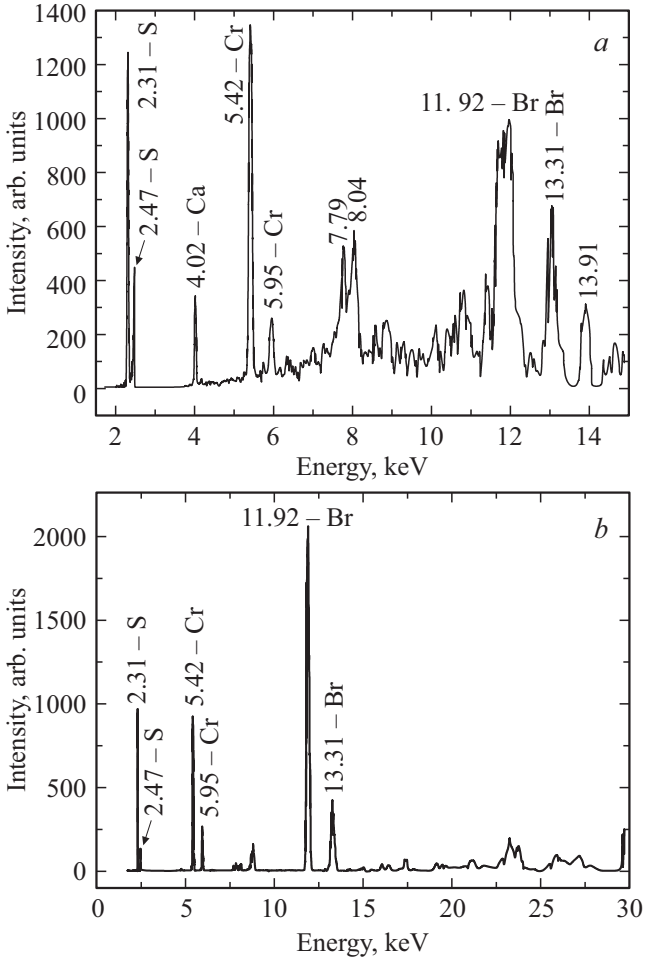

Figure 1. XFA spectrum of sample 1 (*a*) and sample 2 (*b*). al Peaks correspond to the following chemical elements: 2.31 keV — S, 2.47 keV — S, 4.02 keV — Ca, 5.42 keV — Cr, 5.95 keV — Cr, 11.92 keV — Br, 13.31 keV — Br. Peak 7.79 keV may be related to Co, Fe or Ni, peak 8.04 keV corresponds to Cu.

Table 1. Chemical composition of sample 1 in accordance with the XFA data

Chemical element	Atomic concentration, %
S	39.2
Cr	56.0
Br	4.8

Table 2. Chemical composition of sample 2 in accordance with XFA data

Chemical element	Atomic concentration, %
S	32.4
Cr	34.0
Br	33.6

Low content of bromine in sample 1 indicates that this element is an impurity phase component, and the main phase doesn't contain this element. The most probable existing phase may be Cr_2S_3 that has Curie temperature equal to 120 K and that can precisely identify this phase.

Thus, despite the identical chemical composition of the samples as specified by the manufacturers, concentration of elements and atomic structure in them differ considerably.

3.2. Magnetic properties

This section contains the data concerning the magnetic properties of two types of crystals. Figure 2 shows temperature dependences of magnetization (molar susceptibility) of samples 1 (black line) and 2 (red line). It was found that the temperature of transition from a paramagnetic state to a metamagnetic state (Néel temperature) for sample 1

was 120 K, which was much lower than for pure CrSBr (132 K) represented by sample 2. Transition temperature of 120 K corresponds to the bromine-free Cr_2S_3 phase [9,10]. Sample 1 also has a small magnetization maximum at 132 K (Figure 2). Thus, sample 1 primarily consists of the Cr_2S_3 phase. The CrSBr phase is also present in sample 1, but its fraction is small.

Chemical and structural measurement show that the transition temperature shift to 120 K in sample 1 compared with 132 K in sample 2 is caused by the fraction of the Cr_2S_3 phase in sample 1. Magnetic moment dependences on the magnetic field for both samples at 2 K, 20 K and 100 K are shown in Figure 3. Hysteresis loops in sample 1 with a coercive force varying in the range of 10–150 Oe are similar to the pure CrSBr phase in sample 2. Nevertheless, saturation fields in samples 1 and 2 are different. Saturation fields equal to 30 kOe at 2 K and to 10 kOe at 100 K, are much higher in sample 2 than fields 0.5–1 kOe at 2–100 K observed in sample 1. This indicates that the anisotropy field in sample 1 is larger than that in sample 2. In addition, a complex field dependence containing „bends“ was observed in sample 1, while such features were not observed in sample 2. The bends are typical of samples containing several phases with different coercive forces.

Note that the Néel temperature shift from 132 K in a perfect sample to 120 K in a sample with defects could have been also explained by the internal pressure that occurs due to lattice distortions induced by impurity atoms that were very much different in sizes from the initial chemical compound atoms. For example, the temperature dependence of magnetization $M(T)$ for sample 1 is similar to the temperature dependences of magnetization for samples where 50–60% of bromine is replaced with chlorine according to the data in [11]. Comparison of these dependences is shown in Figure 4, *a*.

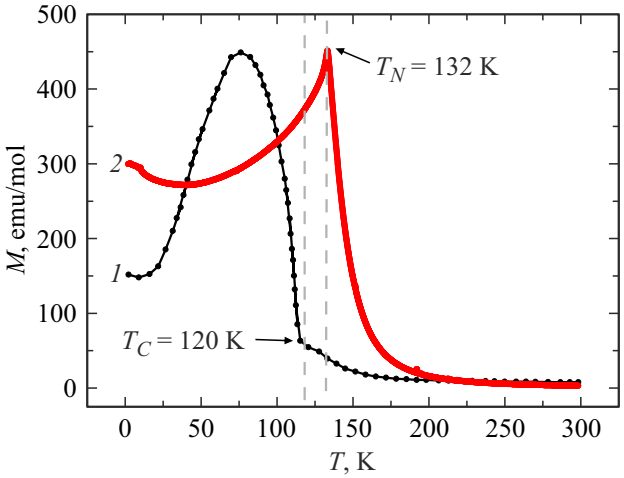

Figure 2. Temperature dependences of magnetization (molar susceptibility) of CrSBr in sample 1 (black line) and sample 2 (red line). Samples were zero-field cooled. Measurement field is 200 Oe and is directed along the *c* axis. Vertical dashed gray lines indicate the Néel temperature of 132 K, known for CrSBr in the literature [11], and the Curie temperature, which is 120 K for Cr_2S3 [9].

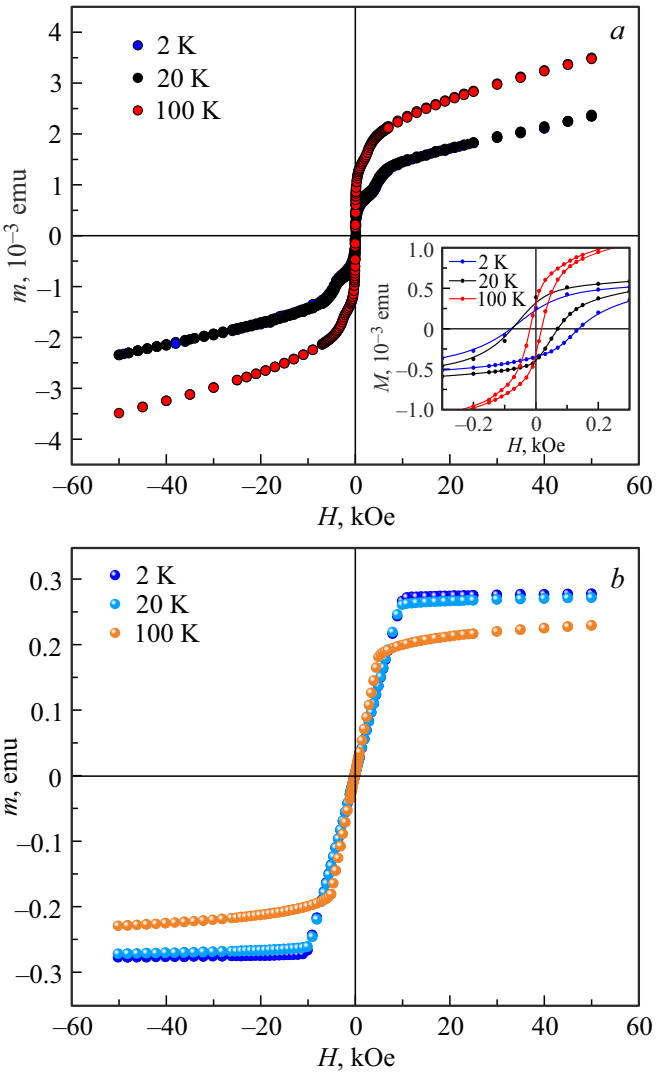

Figure 3. *a* — dependence of the magnetic moment of sample 1 on the field at 2 K, 20 K and 100 K; *b* dependence of the magnetic moment of sample 2 on the field at 2 K, 20 K and 100 K.

Magnetic ordering in CrSBr crystals corresponds to a metamagnetic — ferromagnetic ordering of spins (positive exchange interaction) is observed in layers, and negative exchange interaction takes place between layers so that magnetization directions of the adjacent layers appear to be opposite to each other and compensate each other at low temperatures. This explains the sharp drop of magnetization of such crystals when they are cooled below the Néel temperature. Magnetic state of bulk Cr_2S_3 is called a ferrimagnetic state in many studies [10]. Ferrimagnetic materials are characterized by the presence of two magnetic sublattices with various magnetic moments that are antiparallel, but don't compensate each other, which leads to the total magnetic moment. This ferrimagnetic state may be usually identified by the difference between the

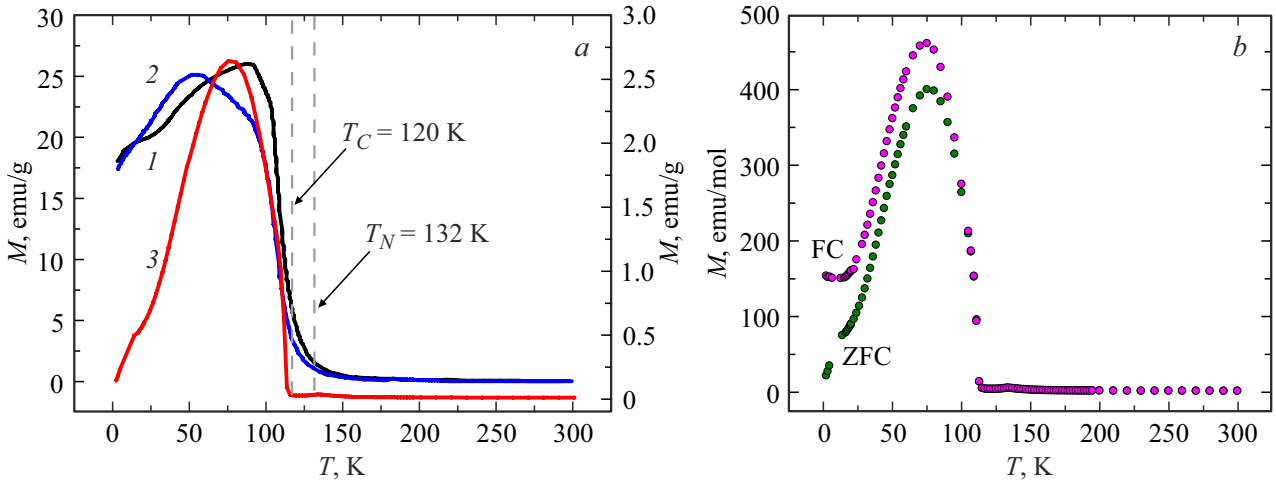

Figure 4. *a* — comparison of temperature dependences of magnetization of test sample 1 measured after zero-field cooling (ZFC), and samples with partial replacement of Br with Cl in [11]: solid black line *1* — a sample with 57% replacement of Cl with Br; solid blue line *2* — sample with 67% replacement of Cl with Br; solid red line *3* — sample 1. *b* — dependence of magnetization of sample 1 on temperature after cooling in 1 T (FC) and 0 T (ZFC) fields. Measurement field — 200 Oe.

temperature dependences of magnetization obtained after zero-field cooling (ZFC) and non-zero-field cooling (FC). In our experiments, ferrimagnetism of the Cr_2S_3 phase was confirmed by comparing curve FC lying above curve ZFC (Figure 4, *b*). In metamagnetic CrSBr crystals, no differences between curves FC and ZFC were observed. These facts also prove that samples 1 have a ferrimagnetic phase, rather than a metamagnetic phase, which is the only phase that should have been observed in CrSBr crystals.

3.3. Raman scattering spectra

Raman scattering spectra characterize lattice vibrations that are sensitive both to the rigidity of interatomic bonds and to the weight of atoms constituting the lattice. Due to this, the RS spectra are sensitive to the absence or replacement of chemical elements, to formation of various phases, and they usually demonstrate the variation of vibration frequencies and of the corresponding position of lines in spectra. Broadening of lines in the Raman scattering spectra often occurs due to lattice nonuniformity induced by defects. Therefore, in addition to peak positions, peak width is also informative, if this involves comparison of imperfect and perfect crystals as in this work.

Before the RSS measurements, bulk crystals were split mechanically to remove the surface layers. After mechanical separation of sample 1, two types of crystals of different shapes were found: rectangular plates of sample 1, which were also obtained when sample 2 was split, and shapeless flakes.

Figure 5, *a* shows the RS spectrum of sample 1 on flakes that differ visually from CrSBr slices with square angles. Five peaks were always recorded for the flakes. Red vertical dashed lines show the peaks corresponding to the pure CrSBr sample [11], blue vertical lines show the RS spectrum of the Cr_2S_3phase [12]. Thus, the measured spectrum contains peak P1 corresponding to the CrSBr spectrum, peaks P3 and P7 corresponding to the Cr_2S_3 spectrum, and peaks P4, P5 and P8, P9 formed by the combination of CrSBr and Cr_2S_3 lines. Peaks P2 and P6 were very small and noisy, and were not included in the discussion. Centers and widths of peaks are listed in Table 3. Lines of peaks P4, P5 and P8, P9 corresponding simultaneously to two phases are wider than the rest lines related to individual phases (Table 3). Line broadening is caused by overlapping of two phase spectra.

Figure 5, *b* shows the RS spectrum of sample 1 in the range of 100–400 cm^{-1}. Three peaks typical of the orthogonal orientation (parallel to the crystallographic *b* axis) are distinguished in this range. These peaks correspond to the out-of-plane vibrations of Br, S and Cr atoms in the lattice. The effect of interlayer vibrations of bromine

Table 3. RS spectroscopy data or sample 1 and data for CrSBr taken from the literature

Peak	CrSBr [11]	Cr_2S_3 [12]	Position of the peak in flakes center of the sample 1	Width of peak in flakes line of the sample 1, cm^{-1}
P1	112	–	114.1	7.32
P2		175.1	–	–
P3		184.8	192.5	7.26
P4	242	–	245	8.11
P5		250.1		
P6		283.1	–	–
P7		308.7	298	7.17
P8	341	–	341.8	8.92
P9		341.8		
P10		360.2	–	–

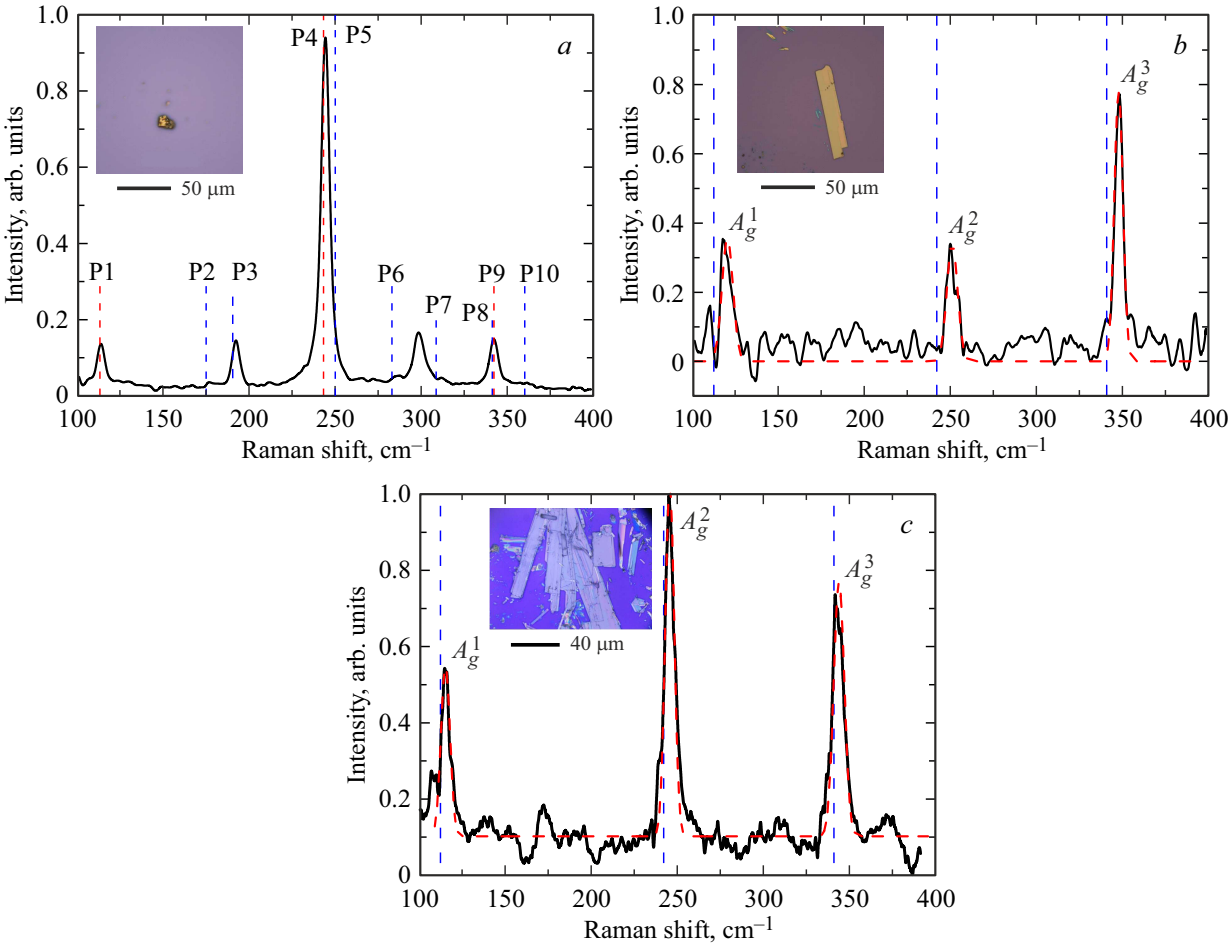

Figure 5. *a* — RS spectrum of shapeless flakes of sample 1. Red dashed lines — positions of peaks for pure CrSBr taken from [11]. Blue dashed lines — positions of peaks for pure Cr_2S_3 taken from [12]. Peak P1 corresponds to the CrSBr spectrum, peaks P3, P7 correspond to the Cr_2S_3 spectrum, peaks P4, P5 and P8, P9 are a combination of CrSBr and Cr_2S_3 lines. The insets show microphotographs of the examined fragments extracted from sample powder 1. *b* — RS spectrum rectangular plates of sample 1 recorded with normal laser beam incidence onto the sample surface (black line). *c* — RS spectrum of sample 2 recorded with normal laser beam incidence onto the sample surface (black line). For (*b*) and (*c*), the red dashed line is an approximation of the spectrum by the sum of Gaussian functions, blue dashed lines are positions of peaks taken from the literature for pure CrSBr [11].

atoms decreases from peak A_g^1 to peak A_g^3, while the latter is affected considerably by Cr−S vibrations [13]. Amplitude ratio in sample 1 indicates redistribution of the peak amplitude due to the absence of Cr−Br bonds in the sample. When comparing peak positions with shifts described in the literature [11] (shown in Figure 5 with vertical dashed lines), upward wavenumber deviation of maximum positions by 8 cm^{-1} is observed. This indicates the difference of chemical composition or structure of sample 1 on the standard CrSBr samples.

Figure 5, *c* shows the RS spectrum of sample 2 in the same spectral range. When comparing with the literature data [11], mean deviation of peak positions in this case was less than 3 cm^{-1}, which indicates that the perfection of sample 2 was much better than that of sample 1.

Data on position and width of peaks detected using the approximation by the Gaussian function are shown in Table 4.

Analysis of line widths detected that lines 1 and 2 in the spectra of sample 1 were wider that in sample 2 (Table 4), which is quite expectable because the lack of bromine in sample 1 gave rise to inadvertent formation of another phase inducing numerous defects and irregularities in the sample. Moreover, co-existence of two Cr_2S_3 and CrSBr phases in sample 1 also leads to broadening of lines in the spectrum compared with single-phase sample 2.

Figure 6, *a* and *b* show Raman scattering spectra of sample 1 and sample 2 (respectively) for various sample rotation angles with respect to the light polarization plane (in 30° steps). It can be seen that the presence of three lines in the spectrum is not observed for all angles, and line amplitudes may differ very much at different rotation angles.

Thus, it was detected that sample 1 consisted of two various microparticles with different shapes (insets in Figure 5, *a* and *b*). Shapeless flakes demonstrate five RS peaks indicating the Cr_2S_3 phase. Rectangular scales in

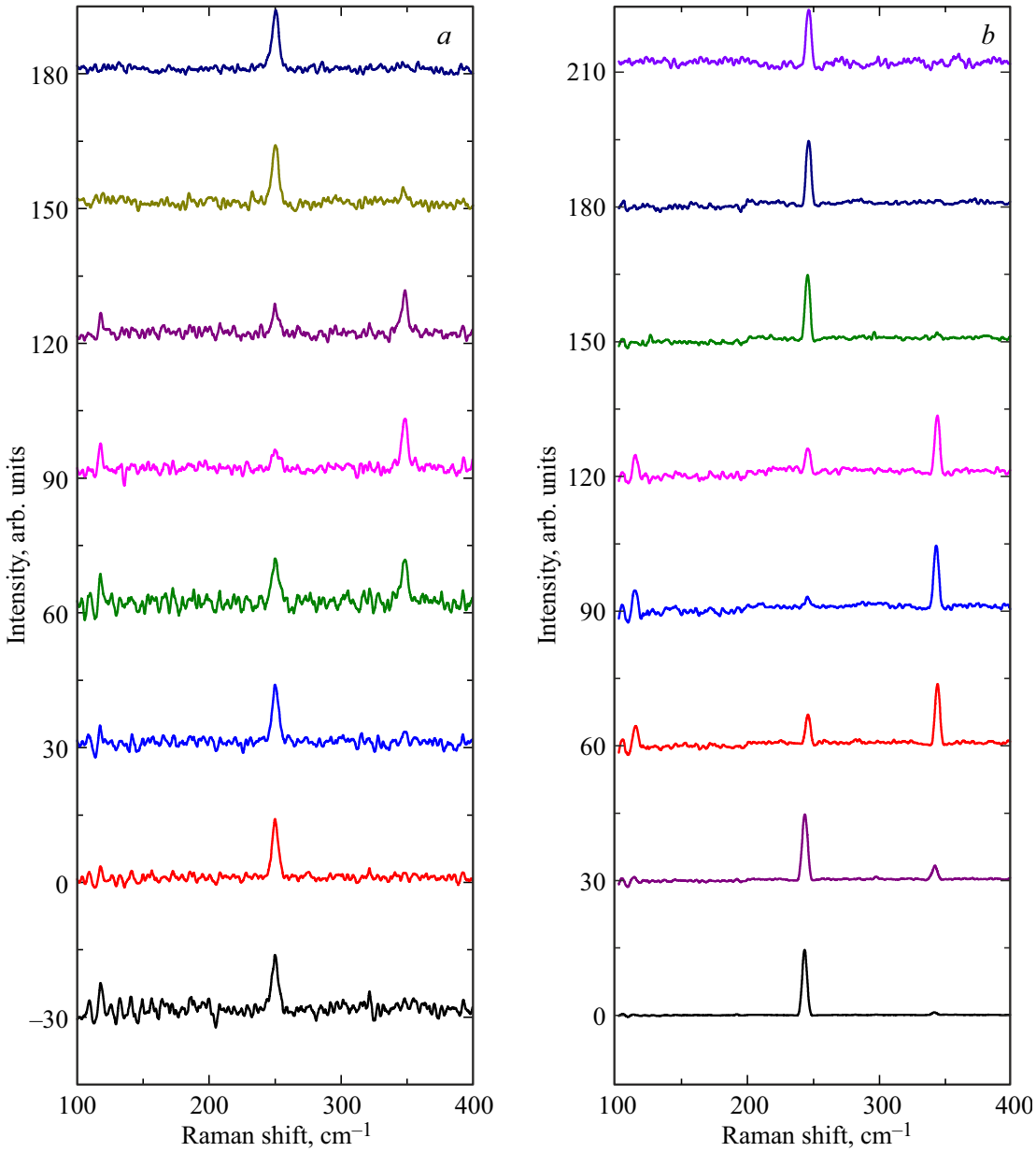

Figure 6. RS spectra for various angles between the light polarization plane and the a axis in sample 1 (a) and sample 2 (b). Angle values in degrees are marked near the spectra.

Table 4. RS spectroscopy data for samples 1 and 2

		Sample 1	Sample 2	CrSBr from the literature [12]
A_g^1	Peak position, cm^{-1} Peak width, cm^{-1}	120 7.803	115 7.416	112 –
A_g^2	Peak position, cm^{-1} Peak width, cm^{-1}	251 7.661	245 6.515	242 –
A_g^3	Peak position, cm^{-1} Peak width, cm^{-1}	348 6.045	344 7.559	341 –

sample 1 correspond to the CrSBr phase that has three peaks in the RS spectrum (Figure 4, *b*). Thus, morphology of microparticles in sample powder 1 allows distinguishing of the CrSBr and Cr_2S_3 phases. Taking into account the magnetic properties of bulk sample 1, potential existence of the Cr_2S_3 phase in the volume is suggested, but when split and in environmental conditions, this phase is instable and forms individual crystals. Actually, CrSBr scales can be still identified after mechanical splitting of bulk sample 1.

4. Conclusions

Comparative analysis of two commercial CrSBr samples with identical specified composition detected differences in the chemical composition and magnetic properties. Our results show that the lack of bromine may give rise to the Cr_2S_3 phase. In a sample with normal content of bromine detected using XFA, the magnetic transition temperature of 132 K corresponds to the values specified in the literature for CrSBr. On the contrary, the sample with low content of bromine demonstrates considerable variation of critical Néel temperature to 120 K followed by Raman scattering spectra variations compared with the reference sample.

Funding

The study was carried out within thematic map 124013100858-3 of the Federal Research Center of Problems of Chemical Physics and Medical Chemistry of RAS.

Conflict of interest

The authors declare that they have no conflict of interest.

References

[1] S.N. Kajale, J. Hanna, K. Jang, D. Sarkar. Nano Res. **17**, 743 (2024).
[2] F. Long, M. Ghorbani-Asl, K. Mosina, Y. Li, K. Lin, F. Ganss, R. Hübner, Z. Sofer, F. Dirnberger, A. Kamra, A.V. Krasheninnikov, S. Prucnal, M. Helm, Sh. Zhou. Nano Lett. **23**, *18*, 8468 (2023).
[3] R. Araujo, J. Zarpellon, D. Mosca. J. Phys. D: Appl. Phys. **55**, 283003 (2022).
[4] K. Bender, K. Dietz, H. Endres, H.W. Helberg, I. Hennig, H.J. Keller, D. Schweitzer. Mol. Cryst. Liq. Cryst. **107**, *1–2*, 45 (1984).
[5] Daniel B. Straus, Cherie R. Kagan. Annual Review of Physical Chemistry **73**, 403–428 (2022).
[6] M. Velický, P.S. Toth, A.M. Rakowski, A.P. Rooney, A. Kozikov, C.R. Woods, A. Mishchenko, L. Fumagalli, J. Yin, V. Zólyomi, T. Georgiou, S.J. Haigh, K.S. Novoselov, R.A.W. Dryfe. Nat. Commun. **8**, 14410 (2017).
[7] K.S. Kim, J. Kwon, H. Ryu, Ch. Kim, J.Ch. Kim, E.-K. Lee, D. Lee, S. Seo, N.M. Han, J.W. Suh, J. Kim, M.K. Song, S. Lee, M. Seol, J. Kim. Nat. Nanotechnol. **19**, 895 (2024).
[8] K. Nandan, A. Agarwal, S. Bhowmick, Y.S. Chauhan. Front. Electron. **4**, 1277927 (2023).
[9] S. Zhou, R. Wang, J. Han, D. Wang, H. Li, L. Gan, T. Zhai. Adv. Funct. Mater. **29**, 1805880 (2019).
[10] W. Su, A. Kuklin, L.H. Jin, D. Engelgardt, H. Zhang, H. Ågren, Y. Zhang. Adv. Sci. **11**, 2402875 (2024).
[11] E.J. Telford, D.G. Chica, M.E. Ziebel, K. Xie, N.S. Manganaro, C. Huang, J. Cox, A.H. Dismukes, X. Zhu, J.P.S. Walsh, T. Cao, C.R. Dean, X. Roy. Adv. Phys. Res. **2**, 2300036 (2023).
[12] A. Gayen, G.H. An, I.N. Rahman, M. Choi, Q. Mustaghfiroh, P.V. Gaikwad, E.S.H. Kang, K.-H. Kim, Ch. Liu, K.W. Kim, J. Bang, H.S. Lee, D.-H. Kim. Nanoscale **16**, 17452 (2024).
[13] K. Torres, A. Kuc, L. Maschio, T. Pham, K. Reidy, L. Dekanovsky, Z. Sofer, F. Ross, J. Klein. Adv. Funct. Mater. **33**, 2211366 (2022).

Translated by E.Ilinskaya